Separation Science and Technology
Publication details, including instructions for authors and subscription information:
http://www.informaworld.com/smpp/title~content=t713708471

Uptake of Ni(II) Ions from Aqueous Solution by Kaolinite and Montmorillonite: Influence of Acid Activation of the Clays

Krishna G. Bhattacharyya[a]; Susmita Sen Gupta[b]
[a] Department of Chemistry, Gauhati University, Guwahati, Assam, India [b] Department of Chemistry, B N College, Dhubri, Assam, India

To cite this Article Bhattacharyya, Krishna G. and Gupta, Susmita Sen(2008) 'Uptake of Ni(II) Ions from Aqueous Solution by Kaolinite and Montmorillonite: Influence of Acid Activation of the Clays', Separation Science and Technology, 43: 11, 3221 — 3250

To link to this Article: DOI: 10.1080/01496390802219638

URL: http://dx.doi.org/10.1080/01496390802219638

Separation Science and Technology, 43: 3221–3250, 2008
Copyright © Taylor & Francis Group, LLC
ISSN: 0149-6395 print/1520-5754 online
DOI: 10.1080/01496390802219638

Uptake of Ni(II) Ions from Aqueous Solution by Kaolinite and Montmorillonite: Influence of Acid Activation of the Clays

Krishna G. Bhattacharyya[1] **and Susmita Sen Gupta**[2]
[1]Department of Chemistry, Gauhati University, Guwahati, Assam, India
[2]Department of Chemistry, B N College, Dhubri, Assam, India

Abstract: Kaolinite and montmorillonite were treated with 0.25 M H_2SO_4 and the acid activated clays along with the parent clays were tested for their uptake capacity for Ni(II) ions from aqueous solution. The batch adsorption experiments were conducted under a set of variables (concentration of Ni(II) ion, amount of clay, pH, time and temperature of interaction). Increasing pH favored Ni(II) uptake till the ions were precipitated as the insoluble hydroxides at $pH > 8.0$. The uptake was rapid up to 40 min and equilibrium was obtained within 180 min. The kinetics of the process was evaluated by subjecting the results to a number of models like the pseudo-first order, second order, Elovich equation, liquid film diffusion, and intra-particle diffusion and it was found that the data more closely resembled a second order process. The experimental data conformed to both Langmuir and Freundlich isotherms showing that the interactions were mostly chemical in nature. The clays had reasonable monolayer adsorption capacity of 10.4, 11.9, 28.4, and 29.5 mg g^{-1} for kaolinite, acid activated kaolinite, montmorillonite, and acid-activated montmorillonite respectively. Montmorillonite had much better adsorption capacity than kaolinite and the acid activation boosted the adsorption capacity of both kaolinite and montmorillonite. The interactions were exothermic in nature, accompanied by decrease in both entropy and Gibbs energy. The results have established good potentiality for kaolinite, montmorillonite and their acid-activated forms to take up and separate Ni(II) from aqueous medium through adsorption-mediated immobilization.

Keywords: Adsorption, acid-activation, batch, kaolinite, montmorillonite

Received 23 November 2007; accepted 19 February 2008.

Address correspondence to K. G. Bhattacharyya, Department of Chemistry, Gauhati University, Guwahati, Assam, India. Tel: +91 361 2571529; Fax: +91 0361 2570599. E-mail address: krishna2604@sify.com

INTRODCUTION

Ni(II) is one of the most toxic contaminants found in the environment. It is released into the aqueous system from industries that make or use nickel, nickel alloys, or nickel compounds, oil-burning power plants, coal-burning power plants, and trash incinerators, mineral processing, paint formulation, electroplating, porcelain enamelling, etc. The respiratory tract and immune systems are sensitive targets of Ni(II) toxicity. Chronic bronchitis, emphysema, and impaired lung function have been observed in nickel welders and foundry workers. The immune response to nickel is elicited as allergic contact dermatitis, a rash that develops shortly after exposure to metallic nickel or nickel compounds. Moreover, it has been established that the male reproductive system might be a sensitive target of ingested nickel toxicity. The carcinogenic effect of nickel has been well documented in occupationally exposed individuals as long-term exposure to less-soluble nickel compounds resulted in lung cancer (1). USEPA recommends that drinking water levels for nickel should not be more than 0.7 mg/L.

Adsorption has been in use for accumulative separation of toxic metal ions in aqueous medium on a suitable substrate and is one of the most effective and economical techniques (2) for decontamination. It is preferred over processes like reverse osmosis, chemical precipitation, ion exchange, solvent extraction, etc., for its ease of operation and insensitivity towards toxic substances (3). A large number of novel adsorbents have been tested, viz, red mud for Cd(II), Zn(II) (4), activated carbon for Zn(II) (5), coconut coirpith for Cd(II) (6), sawdust for Cr(VI) (7), coconut husk for Ag(I) (8), fly ash for Pb(II) and Cr(VI) (9), low-grade phosphate for Zn(II) and Cd(II) (10), chitosan for Cu(II) (11), modified zeolites for Pb(II) and Cd(II) (12), powdered marble wastes for Al(III) (13), rice bran for Zn(II) (14), etc.

In the natural environment, the clay minerals in soil always help in filtering out the contaminants from water as the runoff infiltrates through the soil. The large specific surface area, chemical and mechanical stability, layered structure, high cation exchange capacity (CEC), tendency to hold water in the interlayer sites, presence of Brönsted and Lewis acidity, etc., have made the clays excellent adsorbent materials (15,16).

Treatment of clay minerals with inorganic acids at high temperature is generally referred to as acid activation, which serves to replace exchangeable cations with H^+ ions. The process is accompanied by dealumination from both tetrahedral and octahedral sites, leaving SiO_4 groups largely intact (17). This process generally increases the surface area and acidity of the clay minerals (18). The surface area and the porosity changes depend on the clay minerals, their chemical composition, the type of cations occupying the interlayer space, the type of the acid, the process temperature and duration, etc. (19). The crystalline structure of kaolinite is transformed into amorphous metakaolin by the action of the acid and additional Al-OH and Si-OH bonds are formed without much deforming the original mineral structure (20). The depopulation of the octahedral layer of montmorillonite may lead to structural decomposition depending on how best the clay can resist the acid attack (21). Acid activation followed by thermal treatment has been known to increase the adsorption capacity (22).

The clays have long been known for efficient removal of metal ions from water. Mellah and Chegrouche (23) have shown that natural bentonite has excellent uptake capacity for Zn(II) from aqueous solution with a maximum Langmuir monolayer capacity of 52.9 mg/g (initial Zn(II) concentration 300 mg/L) at 293 K. Similarly, natural and Na-exchanged bentonites could remove Cr(III), Ni(II), Zn(II), Cu(II), and Cd(II) from aqueous solution with Langmuir monolayer capacity of 49.8, 24.2, 23.1, 30.0, and 26.2 mg/g respectively (24). Kara et al. (25) used sepiolite as an adsorbent for Co(II) with the results indicating spontaneous, physical, and entropically driven interactions. Illite was used as an adsorbent for Cd(II) (26) and the process was found to be dependent on ionic strength, initial concentration of Cd(II) and pH, and it was found that 100% Cd(II) removal was possible at pH 8.0. Acid activated kaolinite and montmorillonite have been shown to be good adsorbents for removal of Pb(II) (27), Fe(III) (28), Cd(II) (29), and Co(II) (30).

The present work has been undertaken to make a comparative study of acid activation on kaolinite and montmorillonite for the removal of Ni(II) from aqueous solution in various environmental conditions.

MATERIALS AND METHODS

Chemicals

Reagent grade H_2SO_4 (E. Merck, India) was used for acid activation of clays. A stock solution containing 1000 mg of Ni(II) per liter was prepared by dissolving $Ni(NO_3)_2 \cdot 6H_2O$ (Qualigens, Mumbai, India) in double distilled water and was used to prepare the adsorbate solutions by appropriate dilution.

Clay Adsorbents

Kaolinite, KGa-1b (K1) and Montmorillonite, SWy -2 (M1) were obtained from the University of Missouri-Columbia, Source Clay Minerals Repository, USA.

Acid-activated kaolinite (K2) and acid-activated montmorillonite (M2) were prepared by the procedure of Espantaleon et al. (31). 20 g of clay (kaolinite and montmorillonite) was refluxed with 200 ml of 0.25 M H_2SO_4 for 3 h and the resulting activated clay was separated by centrifugation, washed repeatedly with water till it was free of SO_4^{2-} and dried at 383 K in an air oven till it reached constant weight. The parent clays and the acid activated clays were calcined at 773 K for 10 h before using them as adsorbents.

Characterization

The adsorbents were characterized with XRD (Phillips Analytical PW 1710, Cu Kα radiations), FTIR (Perkin-Elmer Spectrum RXI, range 4400–440 cm^{-1}), surface area (Sears' method; (32)) and cation exchange capacity (CEC, copper bisethylenediamine complex method; (33)) measurements.

Adsorption Experiments

Before the actual adsorption experiments, blank runs were carried out by taking Ni(II) solutions in the same concentration range (as used in the adsorption experiments) in Erlenmeyer flasks without the clay adsorbents and shaking the same as in the actual experiments. The walls of the flask did not show any measurable adsorption of metal ions. The adsorption experiments were carried out in the same flasks by mixing together 0.1 g of clay (except when effect of clay amount was studied) with 50 ml of aqueous Ni(II) solution. The mixture was agitated in a thermostatic water bath (NSW, Mumbai, India) for a pre-determined time interval. The mixture was centrifuged (Remi R 24, 15000 rpm) and Ni(II) remaining unadsorbed in the supernatant liquid was determined with Atomic Absorption Spectrometry (Varian SpectrAA 220 with air-acetylene oxidizing flame). The pH of the adsorptive solution was adjusted by adding aqueous NaOH or HNO_3 of appropriate concentration in drops.

The standard experimental conditions followed in this work are given in Table 1.

Table 1. Experimental conditions for the adsorption measurements

Type of study	Clay (g/L)	Ni(II) (mg/L)	pH	Temperature (K)	Interaction time (min)
Effect of pH	2	50	1, 2, 3, 4, 5, 6, 7, 8, 9, 10	303	180
Effect of clay amount	2, 3, 4, 5, 6	50	5.7	303	180
Effect of Ni(II) concentration	2	10, 20, 30, 40, 50	5.7	303	180
Kinetics	2	50	5.7	303	20, 40, 60, 90, 120, 150, 180, 240, 300, 360
Isotherm	2	10, 20, 30, 40, 50, 75, 100,150, 200, 250	5.7	303	180
Thermodynamics	2	10, 20, 30, 40, 50	5.7	303, 308, 313	180

RESULTS AND DISCUSSION

Adsorbent Characterization

XRD Measurement

Acid treatment and calcination introduces some changes into the crystal structure of clay minerals. The intensities of the characteristic XRD peaks of the clay minerals were reduced on acidification and also the peaks became widened (34). This implies changes in the regular pattern of the clay structure along with partial destruction compared to the original. The dispersion and amorphization of the acid treated clay minerals are known to give rise to an increase in the very low angle diffraction intensities (35) and a reduction in the corresponding tip widths (36). The following observations can be drawn from the XRD measurements:

1. For the calcined, acid activated montmorillonite, the basal spacing expanded from 4.44 to 4.47 Å ($2\theta = 19.98^\circ$), which was accompanied by a decrease in intensity from 43.06 to 29.09%. In case of the calcined, acid activated kaolinite, widening of the basal spacing was comparatively less prominent (from 4.45 to 4.46 Å; $2\theta = 19.92^\circ$) and the peak intensity changed from 23.14 to 21.32% only.

2. The intensity of most of the XRD peaks of montmorillonite decreased sharply on acid treatment such that both octahedral and tetrahedral sites might have been affected drastically.
3. The relative intensity of a low angle peak occurring at $2\theta = 5.70^\circ$ increased from 1.28 (kaolinite) to 4.44% (acid activated kaolinite). Similar effects were however not very prominent in montmorillonite.
4. Acid activation of montmorillonite yielded two new peaks at 22.91 Å ($2\theta = 3.85^\circ$) and 12.49 Å peak ($2\theta = 7.06^\circ$), which were absent in the untreated montmorillonite. Appearance of new peaks indicated the formation of expansible phases and interlamellar expansion (37).
5. The tip width of the 19.98° peak (2θ) in montmorillonite reduced from 0.32 to 0.30 (acid activated montmorillonite); but this feature has not been observed in acid activated kaolinite.

The XRD measurements showed that the activation with 0.25 M H_2SO_4 influenced the structural properties of both kaolinite and montmorillonite, the latter being affected much more. Similar results have been found earlier with vermiculite, illite, and kaolinite treated with hydrochloric acid (35).

FTIR Measurement

The changes brought about by acid treatment of kaolinite and montmorillonite as observed from XRD measurements were further supported by FTIR measurements. The assignment of FTIR bands to different structural features (38) is summarized below:

Effects of acid-activation on kaolinite

1. All the major OH-stretching bands had reduced intensities after acid treatment with some amount of shift in the frequencies. For example, the 3620 cm^{-1} band had shifted to 3623 cm^{-1} with reduction in intensity from 67.0 to 58.0%, the 3692 cm^{-1} band shifted to 3696 cm^{-1} with reduction in intensity from 76.5 to 57.3%, the 3651 cm^{-1} band shifted to 3653 cm^{-1} with reduction in intensity from 69.1 to 63.6%, etc.
2. Instead of two SiO-stretching bands (1010, 1033 cm^{-1}) as found in the parent kaolinite (K1), acid-activated kaolinite (K2) had only one band at 1033 cm^{-1} with a decrease in intensity from 44.3 to 39.3%.
3. The intensity of OH-bending band (915 cm^{-1}) decreased from 62.7 to 53.8% after acid activation with no shift in frequency.

4. The SiO-bending band at 541 cm^{-1} had shown intensity decrease from 62.2 to 54.5% in acid-activated kaolinite (K2). The band at 471 cm^{-1} had shifted to 469 cm^{-1} with decrease in intensity from 63.6 to 54.8%.
5. The band at 722 cm^{-1} due to the presence of quartz impurity in K1, did not change its position in K2, but the intensity decreased from 63.8 to 56.7%.

Effects of acid-activation on montmorillonite

1. The number of OH-stretching bands was the same for both montmorillonite (M1) and acid-activated montmorillonite (M2) with very little deviation of the band positions. However, all the OH-stretching bands had reduced intensities after acid treatment (3512 cm^{-1}: 76.5 to 65.4%, 3554 cm^{-1}: 77.3 to 66.6%; 3620 cm^{-1}: 74.8 to 64.8% with the band shifting to 3621 cm^{-1}), etc.
2. SiO-stretching band (1033 cm^{-1}) for M2 occurred at the same position as that of M1, but the intensity decreased from 59.3 to 49.6%.
3. The SiO-bending band at 464 cm^{-1} decreased in intensity from 72.1% (M1) to 61.1% after acid-activation. The band at 420 cm^{-1} (71.4%) shifted to 428 cm^{-1} with a decrease in intensity to 64.0%.
4. The band at 722 cm^{-1} due to the presence of quartz in M1, did not change its position in M2; however the band showed a decrease in intensity from 69.8 (M1) to 60.5% (M2).

Farmer (38) designated four bands at 3619, 3653, 3669, and 3695 cm^{-1} (due to OH stretching) as the fingerprint bands of kaolinite. In addition, Farmer (38) had also assigned 1011, 1034, 1105, and 1117 cm^{-1} bands to SiO-stretching frequencies, bands in 912–915 cm^{-1} and 935–940 cm^{-1} to OH bending frequencies and bands in 470–472 cm^{-1} and 540–542 cm^{-1} to SiO bending frequencies. Kaolinite and the modified kaolinites had shown IR absorption bands in all the ranges mentioned above. Acid-activated kaolinite (K2) showed new IR bands at 3643 cm^{-1} and 3665 cm^{-1} (39).

Montmorillonite had two characteristic FTIR regions (18,40), viz.,

1. 3500–3750 cm^{-1} (due to the surface structural OH groups of layered aluminosilicates and adsorbed water) and
2. 400–1150 cm^{-1} (due to lattice vibrations).

Ravichandran and Sivasankar (18) have demonstrated that the IR bands of montmorillonite and vermiculite activated with HCl did not exhibit any significant change from those of the parent clays. Similar results are seen in the present work when activation is carried out with 0.25 M H_2SO_4.

The shifts in the principal IR frequencies and modification of their intensities following acid treatment have proven beyond doubt that there is considerable interaction between H^+ ions and the clay surface (both kaolinite and montmorillonite). The results indicate that the acid activation affected those surface groups whose IR frequencies exhibited maximum shift. Thus, with kaolinite, the OH-stretching bands were the ones most affected by acid treatment and the interaction was therefore at the sites of surface OH groups. For montmorillonite, the SiO-bending frequencies showed maximum shifts ($\sim 8\,cm^{-1}$) while the OH-stretching, OH-bending and SiO-stretching bands had not shifted much due to acid treatment. Therefore, acid activation affected the SiO-stretching bands most.

Surface Area

The specific surface areas of kaolinite (K1), acid-activated kaolinite (K2), montmorillonite (M1) and acid-activated montmorillonite (M2) were found to be 3.8, 15.6, 19.8 and 52.3 m^2/g respectively. Ravichandran and Sivasankar (18) reported a specific surface area of 19.0 m^2/g for montmorillonite, which on treatment with HCl (0.1 to 0.7 M) increased up to188.3 m^2/g. Such high values of specific surface area were not achieved in the present work by treatment with 0.25 M H_2SO_4. The literature describing the effects of acid treatment on the specific surface area of kaolinite is scarce, but the untreated kaolinite was reported to have a specific surface area of 5 to 25 m^2/g (41).

The acid treatment opens up the edges of the platelets resulting in expansion of the surface area and increase in the pore diameter (36). Acid treatment replaces exchangeable cations with H^+ ions with the simultaneous loss of some Al^{3+} and other cations from both tetrahedral and octahedral layers leaving the SiO_4 groups intact (17). This process increases the surface area (18) and the results of the present work are in conformity with this.

Cation Exchange Capacity (CEC)

The CEC measurements showed that kaolinite and montmorillonite had CEC of 0.113 and 1.530 meq/g respectively in agreement with the reported values (42). On acid treatment, the CEC of kaolinite increased by about 8% to 0.122 meq/g while that of montmorillonite increased by 12.0% to 3.410 meq/g. Montmorillonite had thus a significant enhancement in the number of exchange sites following treatment with the acid.

Brönsted and Lewis acid sites are associated with the interlamellar region and the edge sites of clays respectively. The ion exchange capacity of clay minerals is attributed to structural defects, broken bonds, and structural hydroxyl transfers (22). The treatment of the clay with 0.25 M H_2SO_4 results in replacement of a number of different cations with H^+ ions and on subsequent heating and calcination, dehydroxylation occurs leaving behind a number of Lewis acid sites. Much of the increase in CEC in the present work is likely to be due to increase in Lewis acidity as the acid treated clay was calcined at 773 K before CEC measurement.

Adsorption of Ni(II)

Influence of pH

Adsorption of Ni(II) increased almost linearly up to pH 8.0 after which a sudden, sharp increase was observed up to pH 10.0 (Fig. 1). In strongly acidic medium, the number of H_3O^+ ions is much more than the number of hydroxylated Ni(II) ions which can hardly meet the competition and as a result, adsorption was low. Under such conditions, the clay surface is likely to be completely covered with H_3O^+ ions and Ni(II) ions can hardly compete with them for the adsorption sites. With the increase in pH, the number of H_3O^+ ions decrease and the positively charged Ni(II) ions adsorb on the free binding sites of the adsorbents. This is a common observation for all cases of adsorption of metal cations on solid surfaces in media of different acidity-basicity (43).

The rapid increase in adsorption of Ni(II) at pH > 8.0 was most likely to be due to onset of precipitation of the hydroxide with Ni^{2+} and $NiOH^+$ being the dominating species (44,45). This was again confirmed by a blank experiment (Fig. 2).

The results of variation of amount adsorbed with pH (Fig. 1) showed that the net effect of acid activation was to increase the number of adsorption sites for Ni(II) and at any pH, the acid activated clay (both kaolinite and montmorillonite) had a higher adsorption capacity compared to the non-activated clay. Under the experimental conditions, montmorillonite and acid-activated montmorillonite, could remove Ni(II) to the extent of 17.8 and 19.4 mg g^{-1} from a solution of concentration 50 mg/L (pH 8.0). For kaolinites, the respective values were 6.8 mg g^{-1} (kaolinite) and 8.3 mg g^{-1} (acid-activated kaolinite). The two curves in each set (Fig. 1) (kaolinite or montmorillonite) were nearly parallel to one another implying

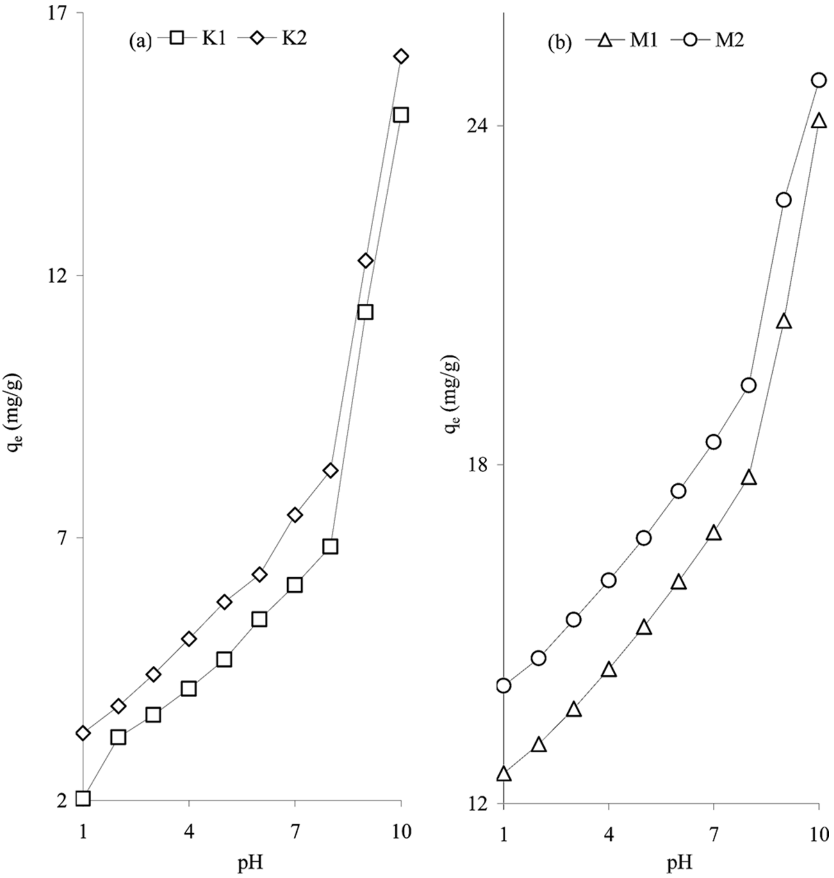

Figure 1. Influence of pH on Ni(II) uptake (mg/g) by (a) kaolinite, K1 and acid-activated kaolinite, K2 (b) montmorillonite, M1 and acid-activated montmorillonite, M2 at 303 K (clay 2 g/L, initial Ni(II) 50 mg/L, time 180 min).

that acid activation enhanced the adsorption capacity uniformly independent of the influence of increasing pH. At any pH, the order of adsorption was acid-activated montmorillonite (M2) > montmorillonite (M1) > acid-activated kaolinite (K2) > kaolinite (K1).

Influence of Interaction Time and Kinetics of Ni(II) Adsorption

Ni(II) uptake continuously increased with time till 180 min after which the increase was insignificant (Fig. 3). The uptake was rapid up to 40 minutes and then, it slowed down as equilibrium was approached

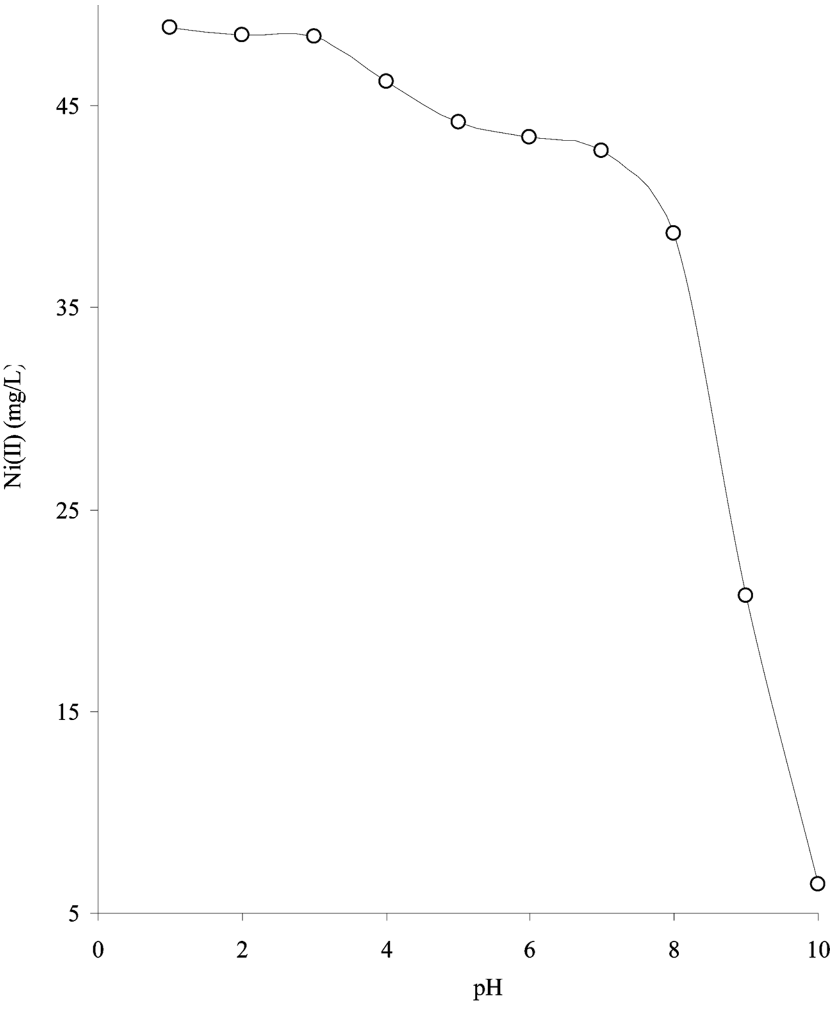

Figure 2. Change of concentration of Ni(II) with increase in pH without clays (Initial Ni(II) 50 mg/L).

(pH = 5.7). During the experiment, initial and final pH values were measured which do not change much. At the onset of the adsorption process, i.e., at low coverage, removal of Ni(II) was very rapid, but as the coverage increased, the number of available surface sites came down, and the rate decreased till equilibrium was attained. At equilibrium, the uptake was controlled by the rate at which the metal ions were transported from the external surface to the interior sites of clay (46).

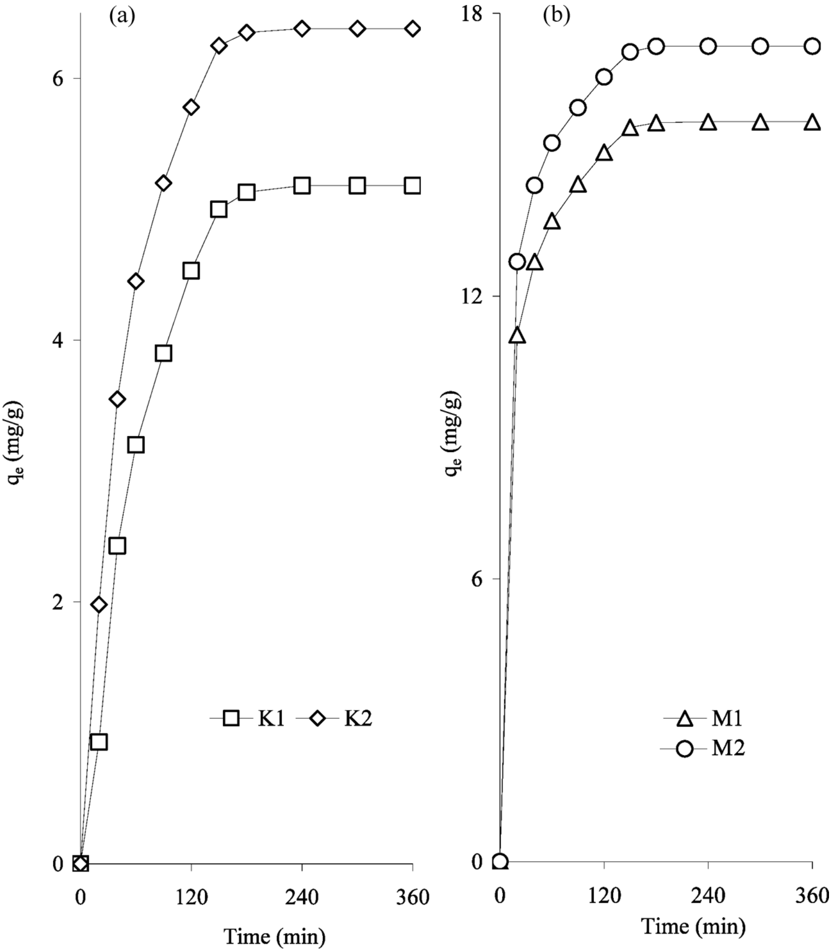

Figure 3. Influence of interaction time on Ni(II) uptake (mg/g) by (a) kaolinite, K1 and acid-activated kaolinite, K2 (b) montmorillonite, M1 and acid-activated montmorillonite, M2 at 303 K (clay 2 g/L, initial Ni(II) 50 mg/L, pH 5.7).

Different models had been used to test the kinetics of clay-Ni(II) interactions. The Lagergren curves were obtained by plotting log ($q_e - q_t$) vs. time according to the pseudo first order kinetic model (47,48),

$$\ln(q_e - q_t) = \ln q_e - k_1 t \tag{1}$$

where q_e and q_t were the amounts adsorbed per unit mass at equilibrium and at any time t, and k_1 was the first order adsorption rate coefficient. The curves were linear (r ~ −0.96 to −0.98) and the first order rate coefficient (obtained from the slopes) varied between 2.6×10^{-2} to $3.1 \times 10^{-2} \text{min}^{-1}$ for the four adsorbents (Table 2). However, linearity of the Lagergren plots does not necessarily assure a first order mechanism (49), which is mainly due to the inherent disadvantage of correctly estimating the equilibrium adsorption capacity, q_e. The q_e values obtained from the Lagergren plots differed from the experimental q_e values from −25.4% to +82.8% (Table 3). With such huge margins of error, the first order kinetics is not the mechanism to explain the rate processes.

The second order rate equation (50), given by

$$t/q_t = 1/(k_2 q_e^2) + (1/q_e)t \tag{2}$$

where $k_2 q_e^2$ is described as the initial adsorption rate as $t \rightarrow 0$. The plots of t/q_t vs. t (Fig. 4), which allowed computation of q_e and k_2, were linear ($r \sim +0.99$) and the rate constant, k_2, varied from 2.2×10^{-2} to 5.5×10^{-2} g $\text{mg}^{-1} \text{min}^{-1}$ (Table 2). A comparison of q_e values (experimental and those obtained from the slopes of the second order plots) now showed a better agreement (Table 3) and the maximum deviation between the two sets of values varied from +4.6% to +30.7%. Deviations still remaining have to be explained on the basis of the rate not following simple second order kinetics.

Table 2. Rate coefficients for Lagergren first order, second order, Elovich equation, intra-particle and liquid film diffusion models for adsorption of Ni(II) on clays at 303 K (clay 2 g/L, initial Ni(II) 50 mg/L, pH 5.7; units for k_1, k_2, α, β, k_i and k_{fd} are min^{-1}, g $\text{mg}^{-1} \text{min}^{-1}$, g $\text{mg}^{-1} \text{min}^2$, mg $\text{g}^{-1} \text{min}^{-1}$, mg g^{-1} $\text{min}^{-0.5}$ and min^{-1}, respectively)

Parameters		Clay adsorbent			
		K1	K2	M1	M2
Lagergren first order	$k_1 \times 10^2$	2.6	3.1	3.1	3.1
	r	−0.98	−0.97	−0.97	−0.96
Second order	$k_2 \times 10^2$	2.2	2.5	5.3	5.5
	r	+0.99	+0.99	+0.99	+0.99
Elovich coefficient	$\alpha \times 10^4$	23.8	85.1	382.8	2267.5
	β	1.8	1.9	1.9	2.0
	r	+0.99	+0.99	+0.99	+0.99
Intra-particle diffusion	$k_i \times 10$	3.9	4.0	4.2	4.2
	Intercepts	−0.1	+0.9	+10.0	+11.6
	r	+0.95	+0.94	+0.95	+0.95
Liquid film diffusion	$k_{fd} \times 10^2$	2.6	3.0	3.1	2.5
	Intercepts	−0.6	−0.6	+0.3	+0.7
	r	+0.98	+0.97	+0.97	+0.97

Table 3. Experimental and computed q_e values from Lagergren and second order plots for adsorption of Ni(II) on clays at 303 K (clay 2 g/L, initial Ni(II) 50 mg/L, pH 5.7)

	q_e (mg/g)				
				Deviation (%)	
Clay adsorbent	Experimental	Lagergren plots	Second order plots	Lagergren plots	Second order plots
K1	5.2	9.4	6.8	+80.7	+30.7
K2	6.4	11.7	8.0	+82.8	+25.0
M1	15.7	12.7	16.5	−19.1	+5.1
M2	17.3	12.9	18.1	−25.4	+4.6

Since second order kinetics in case of chemisorption on energetically heterogeneous solid surfaces also follow the Elovich equation (51,52), given by,

$$q_t = \beta \ln(\alpha\beta) + \beta \ln t \tag{3}$$

the same was applied to the data in the present work. The Elovich plots of q_t vs. ln t were linear ($r \sim +0.99$). The Elovich coefficients, α and β, the initial adsorption rate (g mg^{-1} min^{2}) and the desorption coefficient (mg g^{-1} min^{-1}) respectively had values in the ranges α: 23.8×10^{-4} to 2267.5×10^{-4} g mg^{-1} min^{2} and β: 1.8 to 2.0 mg g^{-1} min^{-1} (Table 2). The acid activated forms had higher α values than that that of the non-activated ones, indicating the formation of comparatively larger number of chemisorptive bonds between acid-activated clays and Ni(II) ions than in case of non-activated clays and Ni(II). The other coefficient, β, did not show any variation among the non activated and acid activated clay adsorbents.

In order to establish whether the rate processes were influenced by diffusion into the pores or diffusion from the bulk solution to the clay surface, two other models were tested for their validity:

1. the intra-particle diffusion plots (q_t vs. $t^{0.5}$) according to the equation (53),

$$q_t = k_i\, t^{0.5} \tag{4}$$

yielded linear curves of $r \sim +0.94$ to $+0.95$, with the rate coefficient, k_i, having values from 0.39 to 0.42 mg g^{-1} $min^{-0.5}$ (Table 2). The plots, however, did not have zero intercept as

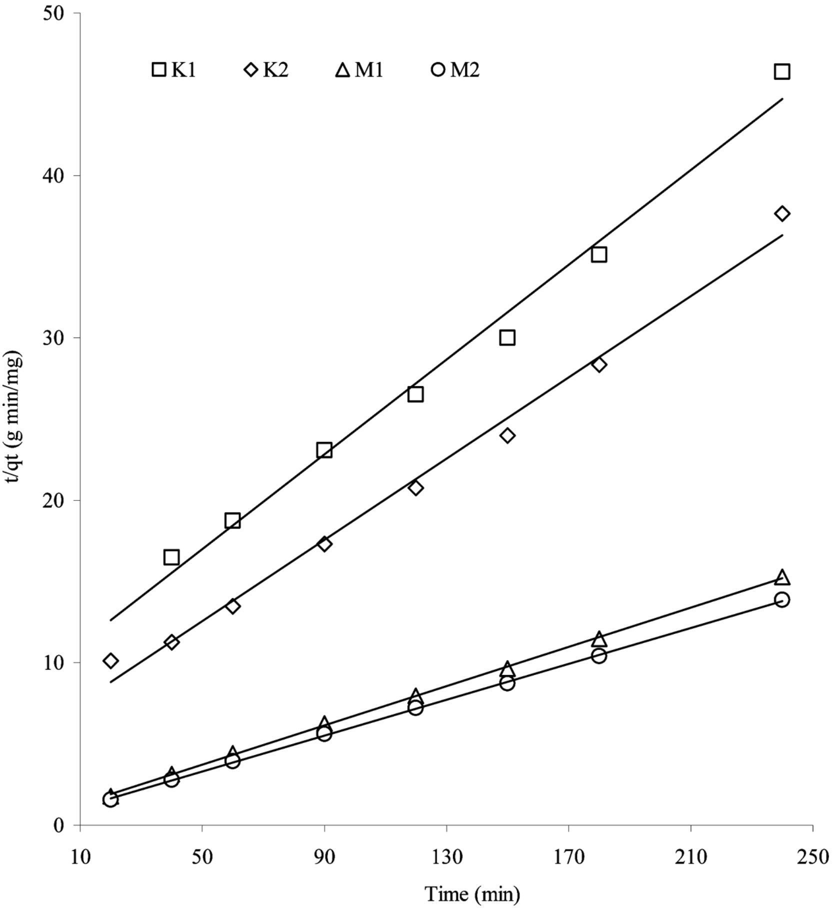

Figure 4. Second order plots for adsorption of Ni(II) on kaolinite K1, acid-activated kaolinite K2, montmorillonite M1 and acid-activated montmorillonite M2 at 303 K (clay 2 g/L, initial Ni(II) 50 mg/L, pH 5.7).

required by the equation (values -0.1 to $+11.6$) indicating that intra-particle diffusion, although could not be ruled out completely, may not be the rate determining factor of the rate processes.

2. The plots as per the liquid film diffusion model (54),

$$\ln(1 - q_t/q_e) = -k_{fd}\ t \tag{5}$$

were also linear ($r \sim +0.97$ to $+0.98$) with intercepts of -0.6 to $+0.7$ (Table 2). The curves did not pass through the origin as required by the model, but the intercepts were close to zero and therefore, diffusion from the liquid phase might have a more significant role than intraparticle diffusion in the kinetics of the adsorption processes. The film diffusion rate coefficient, k_{fd}, had values in the range of 2.5×10^{-2} to $3.1 \times 10^{-2}\ \text{min}^{-1}$ (Table 2).

The kinetics of Ni(II) adsorption on kaolinite, montmorillonite, and their acid-activated forms, as expected is not a simple process and no definite kinetic mechanism could be proposed. The rates are very close to second order kinetics, but other processes may also be operating simultaneously.

Influence of Clay Amount

As the amount of clay was varied from 2 to 6 g/L, Ni(II) adsorption increased from 20.5 to 38.4% for kaolinite, 25.4 to 41.0% for acid-activated kaolinite, 62.8 to 78.4% for montmorillonite, and 69.2 to 85.5% for acid-activated montmorillonite (Ni(II) 50 mg/L). The uptake of Ni(II) per unit mass of the clays (q_e) decreased (Fig. 5) with increase in clay amount. Such results are not uncommon e.g., Cu(II) on sawdust (46); Ni(II) and Cu(II) on natural and acid treated algae (55). The factors, which may be responsible for such behavior, include:

1. When the adsorbent amount is small, the metal ions can easily access the adsorption sites and q_e is high. With increasing adsorbent content, there may be a kind of solid concentration effect when there will be overcrowding of the adsorption sites and although the overall adsorption rises, adsorption per unit mass comes down as the increase is not proportional to the increase in mass.
2. Higher adsorbent amount creates particle aggregation, resulting in a decrease in the total surface area and an increase in the diffusional path length both of which contribute to decrease in amount adsorbed per unit mass (56).

Influence of Initial Concentration of Ni(II)

When the initial concentration of Ni(II) was increased, Ni(II) adsorption came down, and significantly, the uptake per unit mass, q_e increased (Fig. 6).

When the initial metal ion concentration was not high, the ratio of the number of Ni(II) ions to the number of available adsorption sites is small and consequently the adsorption was independent of the initial

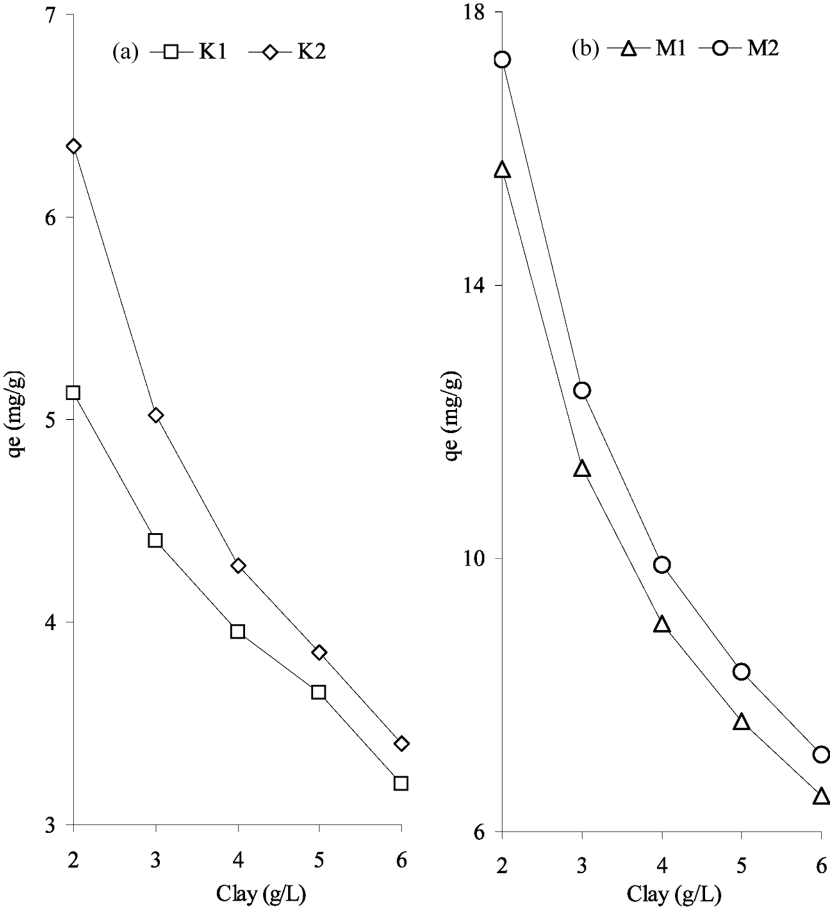

Figure 5. Influence of clay amount on Ni(II) uptake (mg/g) by (a) kaolinite, K1 and acid-activated kaolinite, K2 (b) montmorillonite, M1 and acid-activated montmorillonite, M2 at 303 K (initial Ni(II) 50 mg/L, pH 5.7, time 180 min).

concentration. As the concentration of Ni(II) ions was increased, the competition for adsorption sites became fierce (57) and now, the unit mass of the adsorbent was exposed to a very large number of metal ions. Consequently, the numbers of metal ions taken up by the clays increased as the appropriate binding sites were gradually filled up. This gives rise to an increase in q_e. Similar results have been reported for the removal of other metals on various adsorbents (e.g., Cr(VI) on maple sawdust (7); Ni(II) on almond husk activated carbon (58), etc.).

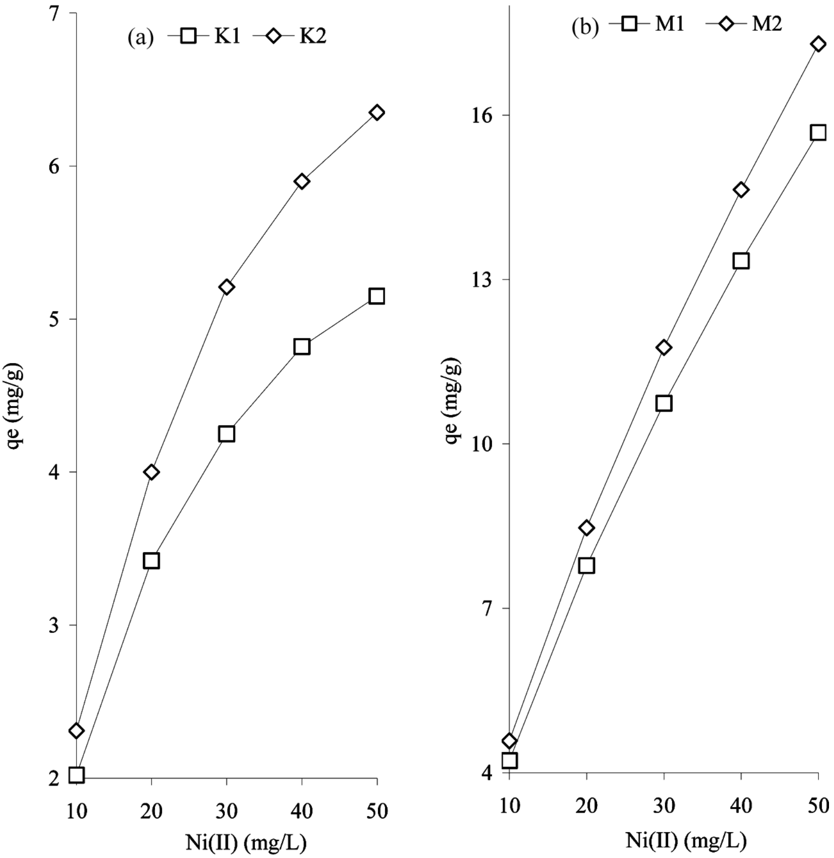

Figure 6. Influence of Ni(II) concentration for adsorption on (a) kaolinite, K1 and acid-activated kaolinite, K2 (b) montmorillonite, M1 and acid-activated montmorillonite, M2 at 303 K (clay 2 g/L, pH 5.7, time 180 min).

As the initial concentration of Ni(II) was varied from 10 to 50 mg/L, the net adsorption of Ni(II) decreased from 40.3 to 20.6%, 46.1 to 25.4%, 84.3 to 62.7%, and 91.5 to 69.2% for kaolinite (K1), acid-activated kaolinite (K2), montmorillonite (M1), and acid-activated montmorillonite (M2), respectively. However, the q_e values increased from 2.0 to 5.2 mg/g for K1, 2.3 to 6.4 mg/g for K2, 4.2 to 15.7 mg/g for M1 and 4.6 to 17.3 mg/g for M2. The order of adsorption among the four clay adsorbents was M2 (acid-activated montmorillonite) > M1 (montmorillonite) > K2 (acid activated kaolinite) > K1 (kaolinite).

Adsorption Isotherm

Freundlich plots, based on the well-known isotherm (59),

$$q_e = K_f C_e^n \tag{6}$$

were linear (r ~ + 0.97 to +0.98) (Fig. 7). This isotherm is generally considered to be applicable to non-specific adsorption on heterogeneous

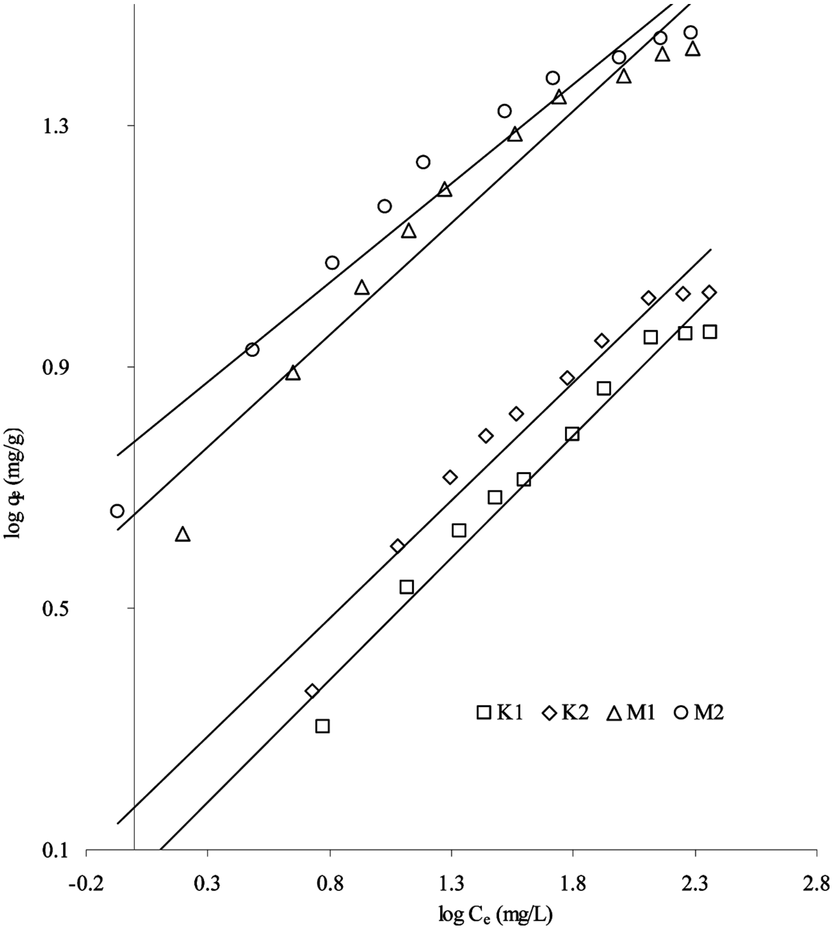

Figure 7. Freundlich plots for Ni(II) adsorbed on kaolinite K1, acid-activated kaolinite K2, montmorillonite M1 and acid-activated montmorillonite M2 at 303 K (clay 2 g/L, initial Ni (II) 10, 20, 30, 40, 50, 75, 100, 150, 200, 250 mg/L, pH 5.7, time 180 min).

solid surfaces. The values of the adsorption coefficients obtained from the plots were given in Table 4. The coefficient, n, varies from 0.3 to 0.4, while the coefficient, K_f was from 1.1 $mg^{1-1/n} L^{1/n} g^{-1}$ (kaolinite, K1) to 6.0 $mg^{1-1/n} L^{1/n} g^{-1}$ (acid-activated montmorillonite, M2). By definition, the adsorption intensity, n, is less than unity and the values obtained in this study conform to the same. The Freundlich adsorption capacity, K_f, was the highest for the acid-activated montmorillonite and the lowest for the non-activated kaolinite. The order of adsorption among the four clay adsorbents was M2 (acid-activated montmorillonite) > M1 (montmorillonite) > K2 (acid activated kaolinite) > K1 (kaolinite).

The Langmuir plots (Fig. 8) obtained from the isotherm (60),

$$C_e/q_e = 1/(bq_m) + (1/q_m)C_e \tag{7}$$

were linear with the regression coefficient, $r \sim +0.99$ (Table 4). Values of b (30.6 Lg^{-1} to 100.2 Lg^{-1}) showed that the equilibrium:

Clay (solid phase) + Ni(II) (aqueous phase)=Clay Ni(II)

was overwhelmingly shifted to the right, i.e. towards the formation of the adsorbate-adsorbent complex. Acid activation resulted in an increase in the Langmuir monolayer capacity, q_m, for both kaolinite and montmorillonite. (q_m for kaolinite and acid-activated kaolinite was 10.4 and 11.9 mg g^{-1}, q_m for montmorillonite and acid-activated montmorillonite was 28.4 and 29.5 mg g^{-1}). The q_m values followed the same order as the Freundlich adsorption capacity, i.e. M2 > M1 > K2 > K1. Kaolinite (1:1 clay) is known to have little isomorphous substitution and consequently, it has lower cation exchange capacity. Isomorphous substitution in both tetrahedral and octahedral layers of montmorillonite (2:1 clay) gives it more surface charge, higher cation exchange capacity and an increased capacity to take up cations (61).

Acid activation enhances Langmuir capacity of kaolinite by ~14.4% (10.4 to 11.9 mg/g), but montmorillonite has only small enhancement (28.4 to 29.5 mg/g). Acid treatment thus generates a considerable number of additional adsorption sites in case of kaolinite, but this influence is not much in case of montmorillonite. It is to be noted that kaolinite, montmorillonite, and their acid-activated forms are calcined at 773 K before carrying out the adsorption of Cd(II) and this might have unequal effects on the adsorption capacities of kaolinite, montmorillonite and their acid-activated forms. Further, acid activation has been known to eliminate mineral impurities from the surface (18) (which might have acted as additional adsorption sites) with partial dissolution of the external layers. This might also be a contributing factor in less-than-expected increase in

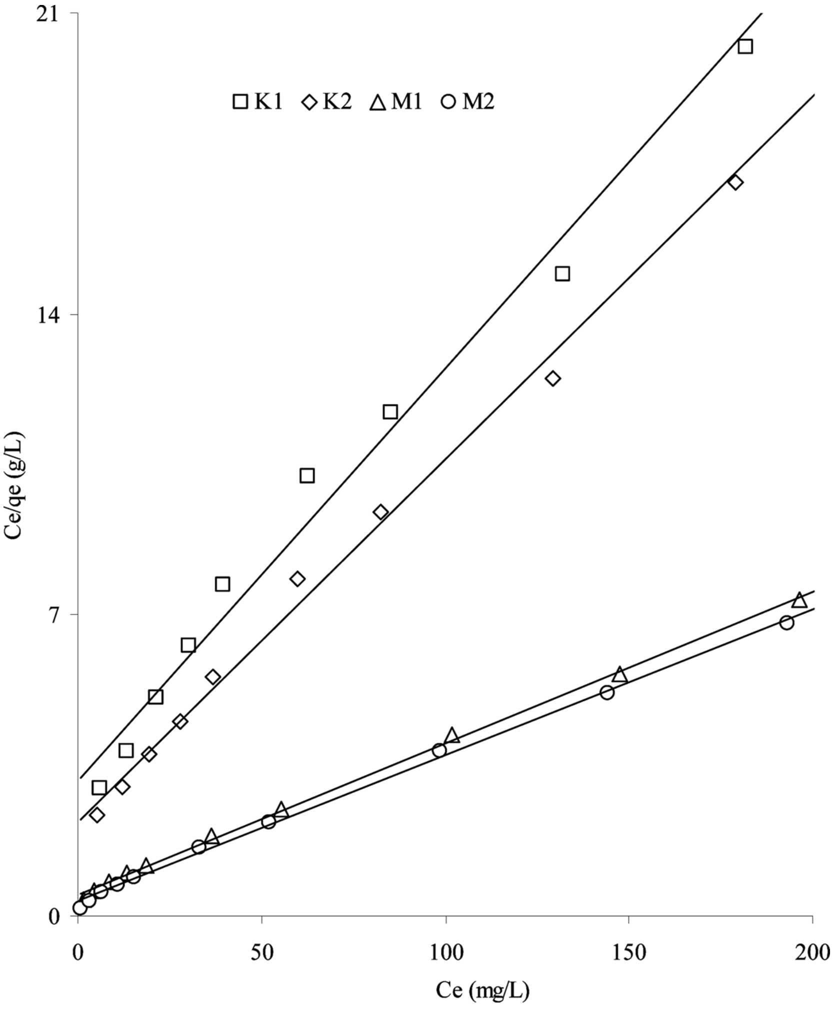

Figure 8. Langmuir plots for Ni(II) adsorbed on kaolinite K1, acid-activated kaolinite K2, montmorillonite M1 and acid-activated montmorillonite M2 at 303 K (clay 2 g/L, initial Ni(II) 10, 20, 30, 40, 50, 75, 100, 150, 200, 250 mg/L, pH 5.7, time 180 min).

adsorption capacity after acid activation. This is also supported by the conclusions already drawn from the FTIR measurements which show that the OH-stretching bands are the ones most affected by acid treatment in kaolinite. The interaction is likely to take place at the sites of these surface OH groups. For montmorillonite, the SiO-bending

Table 4. Freundlich and Langmuir coefficients for adsorption of Ni(II) on clays at 303 K (clay 2 g/L, initial Ni(II) 10, 20, 30, 40, 50, 75, 100, 150, 200, 250 mg/L, pH 5.7, time 180 min; units for K_f, q_m and b are $mg^{1-1/n}L^{1/n}\ g^{-1}$, $mg\ g^{-1}$and $L\ g^{-1}$, respectively).

	Freundlich coefficient			Langmuir coefficient		
Clay adsorbents	K_f	n	r	q_m	b	R
K1	1.1	0.4	+0.98	10.4	30.6	+0.99
K2	1.5	0.4	+0.97	11.9	38. 7	+0.99
M1	4.5	0.4	+0.97	28.4	71.5	+0.99
M2	6.0	0.3	+0.98	29.5	100.2	+0.99

frequencies show maximum shifts ($\sim$8 cm^{-1}) while the OH-stretching, OH-bending and SiO-stretching bands have not shifted much due to acid treatment. Because of this difference in which kaolinite and montmorillonite respond to acid treatment, it is likely that acid treatment does not enhance their adsorption capacity to the same extent.

Values of the adsorption coefficients of Ni(II) on different adsorbents in similar ranges have been reported. The maximum adsorption capacity of Mg-Al-CO_3 hydrotalcite for Ni(II) was reported as 18.0 mg g^{-1} (62). The Langmuir capacity for Ni(II) adsorption on fly ash and two impregnated fly ash samples (impregnated with 0.1 M $Al(NO_3)_3$ or 0.1 M $Fe(Cl)_3$) were reported as 14.0, 15.8, and 14.9 mg g^{-1}, respectively (63). Kumar et al. (64) reported the Freundlich and Langmuir adsorption capacities for Ni(II) on electron beam grafted polymer as 4.3 L g^{-1} and 14.24 mg g^{-1}, respectively.

Influence of Temperature and Adsorption Thermodynamics

The interactions of the metal ions with clay adsorbents in the temperature range of 303 to 313 K were exothermic in nature (Table 5) with the amount of Ni(II) adsorbed on unit mass decreasing from 5.2 to 3.3 mg/g, 15.7 to 12.8 mg/g, 6.4 to 3.7 mg/g and 17.3 to 13.9 mg/g, respectively for kaolinite, montmorillonite, acid-activated kaolinite, and acid-activated montmorillonite. The extent of adsorption (%) showed similar trends. This indicates a tendency of the metal ions to escape from the solid phase to the bulk solution with rise in temperature (65,66) promoting desorption.

The thermodynamic adsorption parameters, ΔH, ΔS, and ΔG (Table 6), were computed from the plots of ln K_d vs. 1/T with the help

Table 5. Effect of temperature on extent of adsorption (%) and amount adsorbed per unit mass (q_e, mg/g) for adsorption Ni(II) on clays (clay 2 g/L, initial Ni(II) 50 mg/L, pH 5.7, time 180 min)

Temperature (K)	Clay adsorbents							
	K1		K2		M1		M2	
	q_e	%	q_e	%	q_e	%	q_e	%
303	5.2	20.6	6.4	25.4	15.7	62.7	17.3	69.2
308	4.2	16.9	4.6	18.5	14.2	56.8	15.4	61.5
313	3.3	13.0	3.7	14.7	12.8	51.3	13.9	55.5}

of the equations (67),

$$\ln K_d = \Delta S/R - \Delta H/RT \tag{8}$$

$$\Delta G = \Delta H - T\Delta S \tag{9}$$

where $K_d(=q_e/C_e)$ is the distribution coefficient of the adsorbate between the solid and the liquid phases (in L/g), T the temperature (K), and $R = 8.314 \times 10^{-3}\,\mathrm{kJ\,K^{-1}\,mol^{-1}}$. The mean adsorption enthalpy, ΔH, had values of -37.9 and $-56.9\,\mathrm{kJ\,mol^{-1}}$ for Ni(II) at equilibrium conditions and at the pH of the solutions as prepared. Although not very high, these values of ΔH can be interpreted on the basis of considerably strong interaction between metal ions and the clays. The adsorption enthalpy increased for both the clays after acid activation, but the increase was much more for montmorillonite, implying that acid activation changed the adsorption sites in such a manner that Ni(II) was held much more strongly to montmorillonite.

Table 6. Thermodynamic data for adsorption Ni(II) on clays (clay 2 g/L, initial Ni(II) 10, 20, 30, 40, 50 mg/L, pH 5.7, time 180 min; units of ΔH, ΔS and ΔG are kJ mol^{-1}, J K^{-1} mol^{-1} and kJ mol^{-1}, respectively)

Parameters		Clay adsorbents			
		K1	K2	M1	M2
$-\Delta H$		37.9	43.1	45.1	56.9
$-\Delta S$		118.2	160.3	146.4	181.9
$-\Delta G$	303 K	41.9	48.1	44.4	55.0
	308 K	42.6	49.4	45.1	55.8
	313 K	43.3	50.3	45.9	56.9

Ni(II)-adsorption on clays was accompanied by an entropy decrease and the mean values varied from -118.2 to $-181.9\,\mathrm{J\ K^{-1}\ mol^{-1}}$. Entropy decrease indicated a positive affinity of the clay minerals towards Ni(II) ions (68) representing a thermodynamically favorable process. As decrease in entropy leads to a stable configuration, the values showed that the adsorption complex between Ni(II) and acid-activated montmorillonite was much more stable when compared with the adsorption complexes between Ni(II) and the other adsorbents. Since stability is associated with an ordered arrangement, it is obvious that the Ni(II) ions in aqueous solution were in a much more chaotic distribution than the Ni(II) ions adsorbed on clays.

All the interactions between clays and Ni(II) led to Gibbs energy decrease, an indication of the spontaneity of the interactions. ΔG values varied from -41.9 to $-43.3\,\mathrm{kJ\,mol^{-1}}$ for kaolinite, -48.1 to $-50.3\,\mathrm{kJ\,mol^{-1}}$ for acid activated kaolinite, -44.4 to $-45.9\,\mathrm{kJ\,mol^{-1}}$ for montmorillonite and -55.0 to $-56.9\,\mathrm{kJ\,mol^{-1}}$ for acid activated montmorillonite.

The thermodynamic data for clay-metal interactions, particularly on acid activated clays are comparatively limited. ΔH, ΔS, and ΔG for adsorption of Ni(II) on illite were of $+16.8\,\mathrm{Kj\,mol^{-1}}$, $+58\,\mathrm{J\,mol^{-1}K^{-1}}$ and $-1.04\,\mathrm{kJ\,mol^{-1}}$ respectively (66). Yavuz et al. (69) had determined ΔH and ΔS values of $+39.52\,\mathrm{kJ\,mol^{-1}}$ and $+11.7\,\mathrm{J\ K^{-1}mol^{-1}}$ for Cu(II), $+37.27\,\mathrm{kJ\,mol^{-1}}$ and $+10.7\,\mathrm{J\ K^{-1}mol^{-1}}$ for Ni(II), $+21.52\,\mathrm{kJ\,mol^{-1}}$ and $+5.4\,\mathrm{J\ K^{-1}mol^{-1}}$ for Co(II) for adsorption on Turkish kaolinite. The ΔH values for Pb(II) interactions on kaolinite, acid-activated kaolinite, montmorillonite, and acid-activated montmorillonite were reported as -33.9, -28.7, -27.6, and $-42.2\,\mathrm{kJ\,mol^{-1}}$, respectively. The corresponding ΔS values were -123.7, -104.5, -86.6, and $-131.8\,\mathrm{J\,K^{-1}\,mol^{-1}}$, respectively (27). All these values compared well with the values obtained in the present work.

CONCLUSIONS

Kaolinite, montmorillonite, and their acid-activated forms are capable of removing Ni(II) from an aqueous solution. Acid activation of the clays enhances their adsorption capacity due to the increased surface area and pore volume. The uptake of Ni(II) by the clay adsorbents increases continuously with pH till precipitation takes over at pH above 8.0.

Ni(II) uptake is very fast initially, but the process slows down later taking time to approach the equilibrium as the diffusion into the interior takes over. The clay-Ni(II) interactions do not follow simple kinetics and although, the second order mechanism gives better compliance with the experimental results, a definite mechanism could not be proposed. The adsorption data agree well with both Langmuir and Freundlich isotherms and the adsorption coefficients support the conditions of favorable adsorption. The interactions are exothermic in nature supported by decreases in both entropy and Gibbs energy.

ACKNOWLEDGEMENTS

One of the authors (SSG) is grateful to the University Grants Commission, New Delhi for providing assistance under the FIP scheme for this work.

GLOSSARY

Symbol	Definition	Units
C_o	initial concentration of the Ni(II)	mg/L
C_e	equilibrium concentration of Ni(II) in liquid phase	mg/L
q_e	equilibrium concentration of Ni(II) in solid phase (i.e. amount of Ni(II) adsorbed per unit mass at equilibrium)	mg/g
q_t	amount of Ni(II) adsorbed per unit mass at any time, t	mg/g
K_f	Freundlich coefficients for adsorption capacity	$mg^{1-1/n} L^{1/n} g^{-1}$
n	Freundlich coefficient for adsorption intensity	
b	Langmuir coefficient for adsorbate-adsorbent equilibrium	$L\ g^{-1}$
q_m	Langmuir monolayer adsorption capacity	$mg\ g^{-1}$
k_1	pseudo first order adsorption rate coefficient	min^{-1}
k_2	second order rate coefficient	$g\ mg^{-1}\ min^{-1}$
k_i	intraparticle diffusion rate coefficient	$mg\ g^{-1}\ min^{-0.5}$
k_{fd}	film diffusion rate coefficient	min^{-1}
ΔH	enthalpy of adsorption	$kJ\ mol^{-1}$
ΔS	entropy of adsorption	$J\ K^{-1}\ mol^{-1}$
ΔG	Gibbs free energy	$kJ\ mol^{-1}$
K_d	distribution coefficient of the adsorbate	$L\ g^{-1}$
T	temperature	K
R	Gas constant	$kJ\ K^{-1}\ mol^{-1}$
r	Regression coefficient	
CEC	Cation exchange capacity	meq/g
K1	Kaolinite	

K2	Acid-activated kaolinite
M1	Montmorillonite
M2	Acid-activated montmorillonite

REFERENCES

1. Draft toxicological profile for nickel, Agency for Toxic Substances and Disease Registry, (http://www.atsdr.cdc.gov), U.S. Department of Health and Human Services: Atlanta, Georgia, 2001.
2. Tran, H.H.; Roddick, F.A.; O'Donnell, J.A. (1999) Comparison of chromatography and desiccant silica gels for the adsorption of metal ions-I. adsorption and kinetics. *Water Res.*, *33*: 2992–3000.
3. Meshko, V.; Markovska, L.; Mincheva, M.; Rodrigues, A.E. (2001) Adsorption of basic dyes on granular activated carbon and natural zeolites. *Water Res.*, *5*: 3357–3366.
4. Gupta, V.K.; Sharma, S. (2002) Removal of cadmium and zinc from aqueous solutions using red mud. *Environ. Sci. Technol.*, *36*: 3612–3617.
5. Ramos, R.L.; Bernal, J.L.A.; Mendoza, B.J.; Fuentes, R.L.; Guerrero, C.R.M. (2002) Adsorption of zinc(II) from an aqueous solution onto activated carbon. *J. Hazard. Mater.*, *B90*: 27–38.
6. Kadirvalu, K.; Namasivayam, C. (2003) Activated carbon from coconut coirpith as metal adsorbent: adsorption of Cd(II) from aqueous solution. *Adv. Environ. Res.*, *7*: 471–478.
7. Yu, L.J.; Shukla, S.S.; Dorris, K.L.; Shukla, A.; Margrave, J.L. (2003) Adsorption of chromium from aqueous solutions by maple sawdust. *J. Hazard. Mater.*, *B100*: 53–63.
8. Hasany, S.M.; Ahmad, R. (2004) Removal of traces of silver ions from aqueous solutions using coconut husk as a sorbent. *Sep. Sci. Technol.*, *39*: 3509–3525.
9. Gupta, V.K.; Ali, I. (2004) Removal of lead and chromium from wastewater using bagasse fly ash–a sugar industry waste. *J. Colloid Interface Sci.*, *271*: 321–328.
10. Kandah, M.I. (2004) Zinc and cadmium adsorption on low-grade phosphate. *Sep. Purif. Technol.*, *35*: 61–70.
11. Verbych, S.; Bryk, M.; Chornokur, G.; Fuhr, B. (2005) Removal of copper(II) from aqueous solutions by chitosan adsorption. *Sep. Sci. Technol.*, *40*: 1749–1759.
12. Wingenfelder, U.; Nowack, B.; Furrer, G.; Schulin, R. (2005) Adsorption of Pb and Cd by amine-modified zeolites. *Water Res.*, *39*: 3287–3297.
13. Ghazy, S.E.; Samra, S.E.; Mahdy, A.M.; El-Morsey, S.M. (2005) Kinetic investigation of the removal of aluminum from water samples by adsorption onto powdered marble wastes. *Sep. Sci. Technol.*, *40*: 1797–1815.
14. Wang, X-S.; Qin, Y.; Li, Z-F. (2006) Biosorption of zinc from aqueous solutions by rice bran: kinetics and equilibrium studies. *Sep. Sci. Technol.*, *41*: 747–756.

15. Tanabe, K. (1981) *Catalysis—Science and Technology*; Anderson, J.R. Boudart, M. (eds.); Springer-Verlag: New York.
16. Naseem, R.; Tahir, S.S. (2001) Removal of Pb(II) from aqueous/acidic solutions by using bentonite as an adsorbents. *Water Res.*, *35*: 3982–3986.
17. Theocharis, C.R.; Jacob, K.J.; Gray, A.C. (1988) Enhancement of Lewis acidity in layer aluminosilicates. *J. Chem. Soc., Faraday Trans.*, *84*: 1509–1516.
18. Ravichandran, J.; Sivasankar, B. (1997) Properties and catalytic activity of acid-modified montmorillonite and vermiculite. *Clays Clay Miner.*, *45*: 854–858.
19. Onal, M.; Sarikaya, Y.; Alemdaroglu, T.; Bozdogan, I. (2002) The effect of acid activation on some physicochemical properties of a bentonite. *Turk. J. Chem.*, *26*: 409–416.
20. Suraj, G.; Iyer, C.S.P.; Lalithambika, M. (1998) Adsorption of cadmium and copper by modified kaolinite. *Appl. Clay Sci.*, *13*: 293–306.
21. Breen, C.; Madejova, J.; Komadel, P. (1995) Correlation of catalytic activity with infra-red, ^{29}Si MAS NMR and acidity data for HCl-treated fine fractions of montmorillonites. *Appl. Clay Sci.*, *10*: 219–230.
22. Rodrigues, M.G.F. (2003) Physical and catalytic characterization of smectites from Boa-Vista, Paraiba, Brazil. *Ceramica 49*: 146–150.
23. Mellah, A.; Chegrouche, S. (1997) The removal of zinc from aqueous solutions by natural bentonites. *Water Res.*, *31*: 621–629.
24. Alvarez-Ayuso, E.; Garcia-Sanchez, A. (2003) Removal of heavy metals from waste waters by natural and Na–exchanged bentonites. *Clays Clay Miner.*, *51*: 475–480.
25. Kara, M.; Yuzer, H.; Sabah, E.; Celik, M.S. (2003) Adsorption of cobalt from aqueous solutions onto sepiolite. *Water Res.*, *37*: 224–232.
26. Echeverria, J.C.; Churio, E.; Garrido, J.J. (2002) Retention mechanisms of Cd on illite. *Clays Clay Miner.*, *50*: 614–623.
27. Bhattacharyya, K.G.; Sen Gupta, S. (2006) Pb(II) uptake by kaolinite and montmorillonite in aqueous medium: influence of acid activation of the clays. *Colloids Surf. A: Physicochem. Eng. Aspects*, *277*: 191–200.
28. Bhattacharyya, K.G.; Sen Gupta, S. (2006) Adsorption of Fe(III) from water by natural and acid activated clays: studies on equilibrium isotherm, kinetics and thermodynamics of interaction. *Adsorption*, *12*: 185–204.
29. Bhattacharyya, K.G.; Sen Gupta, S. (2007) Influence of acid activation of kaolinite and montmorillonite on adsorptive removal of Cd(II) from water. *Ind. Eng. Chem. Res.*, *46*: 3734–3742.
30. Bhattacharyya, K.G.; Sen Gupta, S. (2007) Adsorption of Co(II) from aqueous medium on natural and acid activated kaolinite and montmorillonite. *Sep. Sci. Technol.*, *42*: 3391–3418.
31. Espantaleon, A.G.; Nieto, J.A.; Fernandez, M.; Marsal, A. (2003) Use of activated clays in the removal of dyes and surfactants from tannery waste waters. *Appl. Clay Sci.*, *24*: 105–110.
32. Sears, G.W. (1956) Determination of specific surface area of colloidal silica by titration with sodium hydroxide. *Anal. Chem.*, *28*: 1981–1983.

33. Bergaya, F.; Vayer, M. (1997) CEC of clays: measurement by adsorption of a copper ethylendiamine complex. *Appl. Clay Sci.*, *12*: 275–280.
34. Radojevc, M.; Jovic, V.; Karaulic, D.; Vitorovic, D. (2002) Study of sepiolite from Goles (Kosovo, Yugoslavia). II. Acid activation. *J. Serb. Chem. Soc.*, *67*: 499–506.
35. Jozefaciuk, G.; Bowanko, G. (2002) Effect of acid and alkali treatments on surface areas and adsorption energies of selected minerals. *Clays Clay Miner.*, *50*: 771–783.
36. Diaz, F.R.V.; Santos, P.S. (2001) Studies on the acid activation of Brazilian smectitic clays. *Quim. Nova*, *24*: 345–353.
37. Fanning, D.S.; Keramidas, V.Z.; El-Desosky, M.A. (1989) *Minerals in Soil Environments*; Dixon, J.B.; Weed, S.B. (eds.); Soil Science Society of America, SSSA Book series: Medison, Wisconsin.
38. Farmer, V.C. (1979) *Infrared Spectroscopy*, van Olphen, H.; Fripiat, J.J. (eds.); Data Handbook for Clay Materials and other Non-metallic Minerals, Pergamon Press: Oxford.
39. Johnston, C.T.; Sposito, G.; Bocian, D.F.; Birge, R.R. (1984) Vibrational spectroscopic study of the interlamellar kaolinite-dimethyl sulfoxide complex. *J. Phys. Chem.*, *88*: 5959–5964.
40. Hair, M.L. (1967) *Infrared Spectroscopy in Surface Chemistry*, Marcel Dekker: New York.
41. Volzone, C.; Thompson, J.G.; Melnitchenko, A.; Ortiga, J.; Palethorpe, S.R. (1999) Selective gas adsorption by amorphous clay-mineral derivatives. *Clays Clay Miner.*, *5*: 647–657.
42. Grim, R.E. (1968) *Clay Mineralogy*, McGraw Hill: New York.
43. Padmavathy, V.; Vasudevan, P.; Dhingra, S.C. (2003) Biosorption of nickel-(II) ions on Baker's yeast. *Process Biochem. 38*: 1389–1395.
44. Bayat, B. (2002) Comparative study of adsorption properties of Turkish fly ashes I. The case of nickel(II), copper(II) and zinc(II). *J. Hazard. Mater.*, *B95*: 251–273.
45. Kalyani, S.; Priya, J.A.; Rao, P.S.; Krishnaiah, A. (2005) Removal of copper and nickel from aqueous solutions using chitosan coated on perlite as biosorbent. *Sep. Sci. Technol.*, *40*: 1483–1495.
46. Yu, B.; Zhang, Y.; Shukla, A.; Shukla, S.S.; Dorris, K.L. (2000) The removal of heavy metal from aqueous solutions by sawdust adsorption – removal of copper. *J. Hazard. Mater.*, *B80*: 33–42.
47. Lagergren, S. (1898) Zur theorie der sogenannten adsorption gelöster stoffe. Kungliga Svenska Vetenskapsakademiens. Handlingar., *24* (4): 1–39.
48. Ho, Y.S. (2004) Citation review of Lagergren kinetic rate equation on adsorption reactions. *Scientometrics*, *59*: 171–177.
49. Ho, Y.S.; McKay, G. (1999) The sorption of lead(II) ions on peat. *Water Res.*, *33*: 578–584.
50. Ho, Y.S.; McKay, G. (1999) Batch lead (II) removal from aqueous solution by peat: equilibrium and kinetics. *Trans I Chem E.*, *77B*: 165–173.
51. Ho, Y.S.; McKay, G. (1998) A comparison of chemisorption kinetic models applied to pollutant removal on various sorbents. *Trans I Chem E.*, *76B*: 332–339.

52. Rudzinski, W.; Panczyk, T. (2002) The Langmuirian adsorption kinetics revised: a farewell to the XXth century theories? *Adsorption*, *8*: 23–34.
53. Weber, W.J.; Morris, J.C. (1963) Kinetics of adsorption of carbon from solutions. *J. Sanit. Engg. Div. Am. Soc. Civ. Engg.*, *89*: 31–63.
54. Boyd, G.E.; Adamson, A.W.; Myers, Jr.; L.S. (1947) The exchange adsorption of ions from aqueous solutions by organic zeolites II. Kinetics. *J. Am. Chem. Soc.*, *69*: 2836–2848.
55. Rao, P.S.; Kalyani, S.; Reddy, K.V.N.S.; Krishnaiah, A. (2005) Comparison of biosorption of nickel(II) and copper(II) ions from aqueous solution by Sphaeroplea algae and acid treated Sphaeroplea Algae. *Sep. Sci. Technol.*, *40*: 3149–3165.
56. Shukla, A.; Zhang, Y-H.; Dubey, P.; Margrave, J.L.; Shukla, S.S. (2002) The role of sawdust in the removal of unwanted materials from water. *J. Hazard. Mater.*, *95*: 137–152.
57. Ucun, H.; Bayhan, Y.K.; Kaya, Y.; Cakici, A.; Algurb, O.F. (2003) Biosorption of lead(II) from aqueous solution by cone biomass of Pinus sylvestris. *Desalination*, *154*: 233–238.
58. Hasar, H. (2003) Adsorption of nickel(II) from aqueous solution onto activated carbon prepared from almond husk. *J. Hazard. Mater.*, *B97*: 49–57.
59. Freundlich, H.M.F. (1906) Over the adsorption in solution. *J. Phys. Chem.*, *57*: 385–470.
60. Langmuir, I. (1918) The adsorption of gases on plane surfaces of glass, mica, and platinum. *J. Am. Chem. Soc.*, *40*: 1361–1403.
61. Chantawong, V.; Harvey, N.W.; Bashkin, V.N. (2003) Comparison of heavy metal adsorptions by Thai kaolin and ballclay. *Water Air Soil Pollut.*, *148*: 111–125.
62. Lazaridis, N.K. (2003) Sorption removal of anions and cations in single batch systems by uncalcined and calcined Mg-Al-CO_3 hydrotalcite. *Water Air Soil Pollut.*, *146*: 127–139.
63. Banerjee, S.S.; Jayaram, R.V.; Joshi, M.V. (2003) Removal of nickel(II) and zinc(II) from wastewater using fly ash and impregnated fly ash. *Sep. Sci. Technol.*, *38*: 1015–1032.
64. Kumar, V.; Bhardwaj, Y.K.; Dubey, K.A.; Chaudhari, C.V.; Goel, N.K.; Biswal, J.; Sabharwal, S.; Tirumalesh, K. (2006) Electron beam grafted polymer adsorbent for removal of heavy metal ion from aqueous solution. *Sep. Sci. Technol.*, *41*: 3123–3139.
65. Abou-Mesalam, M.M. (2003) Sorption kinetics of copper, zinc, cadmium and nickel ions on synthesized silico-antimonate ion exchanger. *Colloids Surf. A: Physicochem. Eng. Aspects*, *225*: 85–94.
66. Echeverria, J.; Indurain, J.; Churio, E.; Garrido, J. (2003) Simultaneous effect of pH, temperature, ionic strength, and initial concentration on the retention of Ni on illite. *Colloids Surf. A: Physicochem. Eng. Aspects*, *218*: 175–187.
67. Thomas, W.J.; Crittenden, B. (1998) *Adsorption Technology and Design*; Butterworth-Heinemann: Oxford.

68. Gupta, V.K.; Gupta, M.; Sharma, S. (2001) Process development for the removal of lead and chromium from aqueous solutions using red mud Δ an aluminium industry waste. *Water Res.*, *35*: 1125–1134.
69. Yavuz, O.; Altunkaynak, Y.; Guzel, F. (2003) Removal of copper, nickel, cobalt and manganese from aqueous solution by kaolinite. *Water Res.*, *37*: 948–952.